International Journal of Thin Films Science and Technology

http://dx.doi.org/10.18576/ijtfst/110207

Effect of High Temperature on Thermal Analysis, Structure and Morphology of CeO2 Nanoparticles Prepared by Hydrothermal Method

Hamed A. Gatea

Department of Radiology, College of Health and Medical Technololgy, Al-Ayen University, Thi-Qar, Iraq

Received: 2 Mar. 2022, Revised: 12 Apr. 2022, Accepted: 16 Apr. 2022
Published online: 1 May 2022

Abstract: Cerium oxide(CeO_2) nanoparticles have been prepared by Hydro-Thermal method.The nanoparticles size of cerium oxide was obtained from the solution after drying and heat treatment at a high temperature of 800,900 and 1100 ˚C were in different sizes. The thermal analyses of CeO2 is investigated. The results showed by the x-ray diffractometers that all nanoparticles of cerium oxide have the fluorite crystalline structure. The optical properties showed that the transmittance coefficient decreases with increasing temperatures. There is no significant change in energy band gap where is the increasing sintering temperature.

Keywords: CeO2 nanoparticles, PL spectra, Heat treatment, optical properties.

1 Introduction

Nanostructured materials have garnered considerable interest due to their claimed unique structure and physical properties related to the grain boundary and grain size-dependent non-stoichiometry [1]. According to a number of studies, materials with a grain size of less than 100 nm have distinct optical, electrical, catalytic, and mechanical properties than do ordinary microcrystalline specimens [2,3]. High transparency in the visible and near-IR range, as well as electro-optical performance, have piqued interest in cerium oxide (ceria) films [3,4] . Optical and electrical applications may benefit from using rare earth oxides (e.g. optical filters, capacitors). CeO2 is a fascinating material [5].

Ceria as known or Cerium(IV) oxide is very attractive metal oxides that have more attention at last 10 years because it has unique interesting characteristics, such as good stability at high temperature, reactivity, better hardness and UV absorption [6,7].

CeO2 samples prepared as nanoparticles form have been a wide variety of application such as gas sensors, sunscreen cosmetics, eye disorder, oxygen storage capacity and disease treatment [7,8].

Most new methods applied to prepare CeO_2 nano-particles such as flame spray pyrolysis, hydrothermal synthesis, sol–gel methods, combustion synthesis and a complex thermos-decomposition method [9]. There are many modern methods that are relied to prepare nanoparticles, but there are some problems that exist in these methods, such as the need for high pressure or high temperature, which is complicated, production costs are increasing enormously and not eco-friendly [9-11]. For these reasons using low-cost, nondoxical and ecologically method is important in order to manufacture CeO2 nanoparticles [11-13].

In this work, the method used to prepare CeO2 nanoparticles due to simple method and costly method, and with this method can obtain different size with increasing time example

2 Experimental Sections

“Cerium nitrate (Ce (NO3)2.6H2O) and sodium hydroxide (NaOH)” were used as precursors. [Ce (NO3)26H2O] dissolved in 8 ml distilled water and sodium hydroxide [NaOH] was dissolve 40ml of distilled water.

The first solution (CeO2 nitrate) add to second solution (NaOH) slowly and then the total solution was mixed and stirred 60 min at 60 ˚C. The solution will be transferred to a Teflon-lined autoclave, which maintained a constant pressure and temperature of 150 for a period of 12 hours. The autoclave could naturally cool down and reach the room temperature.

The solution was collected and rinsed with ethanol and distilled water more than once. The solution dried at 120˚C for 4 hours. The powders ground by mortar and pestle to get fine powders. The powder was calcinated at 400 ˚C

*Corresponding author E-mail: hamedalwan14@gmail.com

for 2 hours. After the powder is calcined, the powder is ground again with a mortar and pestle, and then the powder is compacted by a cylindrical press to form a disk in order to use in SEM sample test and other tests. "The thermogravimetric–differential thermal analysis (TG–DTA; PerkinElmer Pyris Diamond)" was used to describe the precursor in order to identify the thermal decomposition and crystallization temperatures. Using powder XRD (D-Bruker advanced diffractometer with a Cu Kα radiation (0.15406 nm), the sintering samples were analyzed for crystal phase identification. Using an Ar laser with an excitation of 514.5 nm, a beam with a diameter between 1 and 2 micrometers was focused on a specimen under a 90x microscope. Scanning Electron Microscopy(SEM Hitachi H 6000, 150 kv) was used to analyze the particle size and morphology of the powder samples. In order to prepare the sample for the study, the significantly weight loss was observed that mean the CeO2 nanoparticles thermal analysis was stable. Organic materials combustion leads to major weight loss, while the minimal weight loss is due to trapped solvents such as mixture was spread out in methanol and the illumination employed for the photoluminescence spectra measurement was 290 nm.

3 Results and Discussion

EDAX studies

Energy Dispersive spectroscopy(EDS) was used to analyze the elements of CeO_2 powders. EDS spectrum of CeO2 powders sintering at 800, 900 and 1100˚C shows in Fig. 1 and Table 1. There were just two lines found: one for Ce and one for O revealed by EDS spectrum. This indicates, the samples doesn't contain any impurities. The atomic ratio of Ce/O and the weight ratio are found in table 1 which prepared at 800,900 and 1100˚C. The existence of Ce and O in the product was confirmed by the EDX

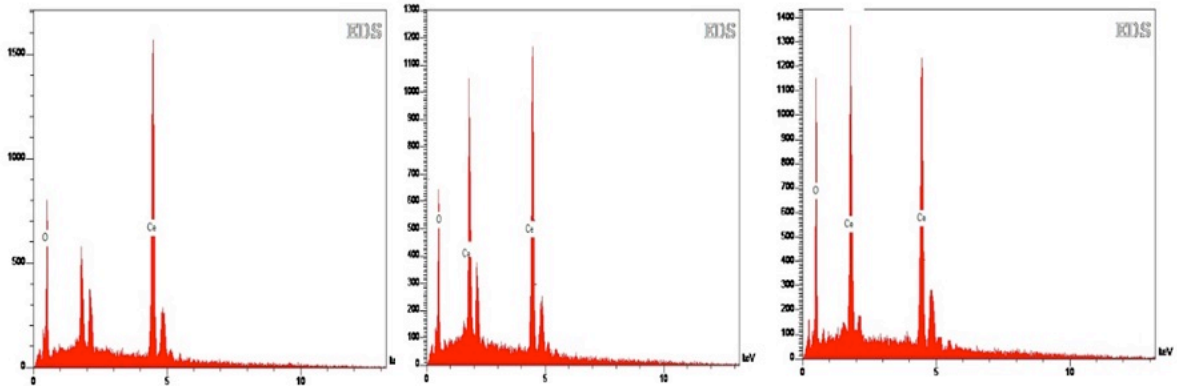

Fig.1: EDX spectra of CeO2 nano-powders with different sintering temperature.

Table 1: The Calculated and experimental values of the element content in Ceo2 nanopowders.

Temperature	Weight %		Atomic %	
˚C	Cerium	Oxygen	Cerium	Oxygen
800	28.16	71.84	4.28	95.72
900	43.01	56.99	7.93	92.07

CeO2 nanoparticle stability was tested at a flow rate of N_2 of 50 milliliters per minute using TGA demonstrates as exhibited in Fig. 2. Fig. 2 shows the behaviour thermal analysis of CeO2 nana powders, CeO_2 nanoparticles thermogram showed that a mass loss between 120 °C and 400 °C was associated with the hydration due to loss of water. The TG curve reveals a minimal weight loss beginning from 70 to 190 °C and a large weight loss beginning from 190 to 390 C. At 200°C, there is no carbon, acetate, and water.

The obvious plateau generated on the TG curve between 390 and 900 °C demonstrates the development of nano-crystalline CeO2. The DTA curve shows, the exothermic point observed between 290 and 330 ˚C, as a result, organic species and precursors were responsible for the thermal events. According to the DTA curve, the endothermic peak

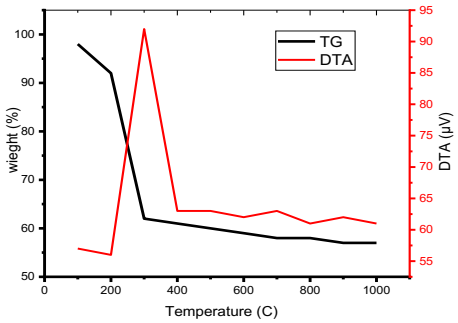

Fig.2: TG–DTA curves of thermal decomposition of nano-crystalline CeO2.

was observed due to the melting process in the range of 216–220 °C. "The thermograms of ligands indicated that the decomposition of the ligands had one step and their weight loss was about 80 percent" [12]. "The melting point of the synthesized ligands was compatible with TGA analysis" [12].

The XRD patterns of CeO2 nanoparticles samples were detected by x-ray diffractometer that show in Fig. 3. "All the sintering samples showed on XRD peaks that correspond to the (111), (200), (220) and (311) planes for a cubic fluorite structure of CeO2 in the standard data (JCPDS:34-0394)"[14]. The increasing sintering temperature leads to the reflection peaks become sharper that clearly revealed enhancement of crystallinity. The effect of high treatment temperature on the inter-planer space (d_{hkl}) listed in Table.2. The powders crystallite size estimated by Scherer's equation were estimated to be 32, 37 and 47 nm for CeO_2 samples sintering at 800, 900 and 1100 ˚C, respectively. The listed all method to calculated particles size on Table .2

The particles size varied with increased sintering temperature, so the lattice parameter calculated using Scherer's equation from the XRD spectra for all CeO_2 samples. The lattice values listed in Table. 3. These values are marginally lower than the CeO2 readings (a= 0.54113) nm. The lattice parameter of nano-crystalline powders has been observed to fluctuate with particle size; this behavior has been explained in terms of grain surface relaxation.

Table 2: Measured inter-planar spacing (d_{hkl}) obtained from samples sintering at 800,900,1100 ˚C.

	(d_{hkl}) Experimental data			Standard data	
No.	**800 ˚C**	**900 ˚C**	**1100 ˚C**	**d_{hkl}**	**hkl**
1	**4.109**	**4.098**	**4.119**	**4.130**	**211**
2	**2.999**	**2.937**	**2.924**	**2.924**	**222**
3	**2.537**	**2.542**	**2.556**	**2.529**	**400**
4	**2.000**	**1.986**	**1.881**	**1.848**	**411**
5	**1.800**	**1.802**	**1.804**	**1.788**	**332**
6	**1.702**	**1.649**	**1.654**	**1.642**	**431**

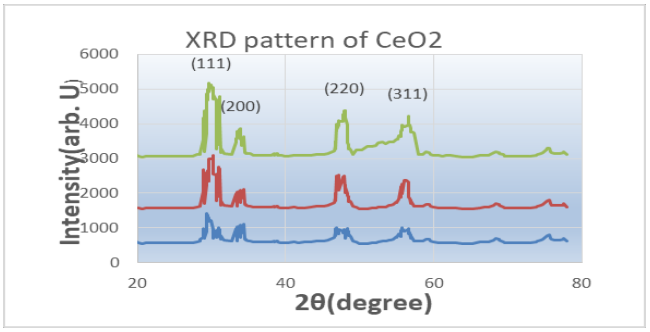

Fig. 3: XRD patterns of nano-crystalline CeO2 sintering at 800,900,1100 ˚C.

Table 3: Average particles size compared between some method and lattice parameters of CeO2 nanopowders sintering at different temperature.

Sintering Tem. ˚C	**Scherres Eq.(nm)**	**Willamson-Hall(nm)**	**From SEM(nm)**	**Lattice parameter**
800 ˚C	**32**	**38**	**54-62**	**0.53755±0.00018**
900 ˚C	**37**	**41**	**90-98**	**0.54093±0.00018**
1100 ˚C	**46**	**53**	**118-122**	**0.54050±0.00018**

The SEM images revealed the structure and morphology of CeO2 nanomaterials samples which sintering at 800,900 and 1100 ˚C. SEM images corresponding pattern of nano-crystalline

CeO2 samples show in Fig. 4.

Through the images shown by scanning electron microscope, it was discovered that increasing the temperature causes an increase in particle size. As shown by images, at low temperatures, all the samples contain a weekly aggregation, while it is stronger at high temperatures because to an increase in density. As expected, the particle size ranges between

118-122 nm at a temperature of 1100 ˚C, while less than that at the remaining temperature calculated by ImageJ program (1.52t version).

Optical Studies

Fig.5 shows, the transmission spectrum of Cerium oxide (CeO2) nano-powders were prepare at different sintering temperatures (800,900 and 1100˚C). The pellet transmittance decreases with increase of sintering temperatures.

The disk of CeO2 nanopowders prepared at 800˚C shows the maximum transmittance of 91.12% at 550 nm. The pellet sintering at 800˚C show higher value of average optical transmittance compared to that of the pellets sintering at 900 and 1100˚C . This can be due to the improved crystallinity. The transmittance data obtained for the samples are used to calculate the absorption coefficients at different wavelengths using the following relation

$$\alpha = \ln\left(\frac{1}{T}\right) t \quad \ldots\ldots(1)$$

Where t is the pellets thickness and T is the transmittance of the samples.

The charge transition occurred from (4f band) to the (valence band) leads to this phenomenon. The crystalline defects in the surface in the CeO2 nanoparticle samples lead to the emission of blue and greenish-blue color[15]. All of the samples had different intensity values in the spectra because of the oxygen vacancies formed during the preparation process. The emission spectrum of a CeO2 sample sintering at 1100 ˚C is greater than that of CeO2 samples sintering at 800 and 900 ˚C. This could imply that the CeO2 sample sintering at 1100 degrees Celsius has superior crystallinity than the other samples.

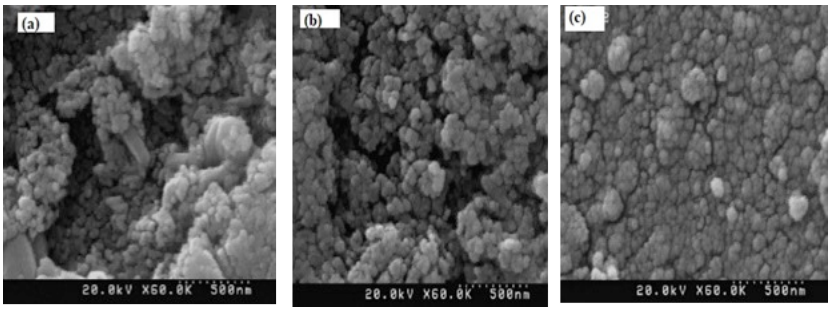

Fig. 4: SEM images of the nano-crystalline CeO_2 samples sintering in air for (3 h) at (a)800, (b) 900, and (c) 1100 °C.

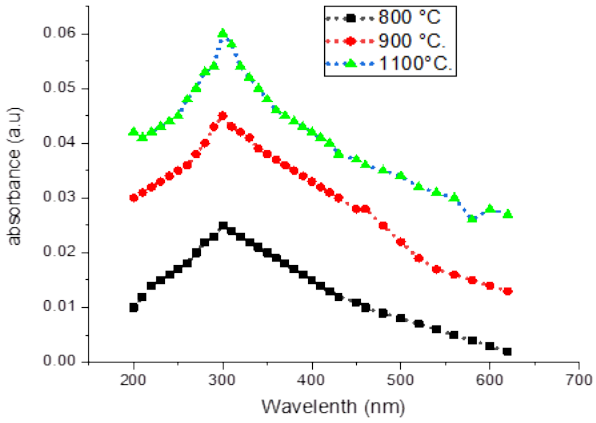

Fig. 5: The absorbance spectra of CeO2 films prepared at the substrate temperatures of 800,900 and 1100 ˚C.

Table 4: Optical parameters of CeO2 nano-powers with different sintering temperature.

Sintering temperatures(˚C)	α (*10^6)	K	Bandgap(eV)	Refractive index	Packing density
800	1.78	0.081	3.66	2.35	0.21
900	1.57	0.0632	3.71	2.11	0.27
1100	1.39	0.0408	3.73	2.08	0.36

The following equation used to estimate optical band gap by the Tauc plot [11]

$$\alpha h\nu = A(h\nu - Eg)m \ldots\ldots(2)$$

"Where A is a constant, hν is the photon energy and m depends on the nature of optical transition. The value of m is (½) for direct allowed, 2 for indirect allowed". The Fig. 6 shows the (αhν)2 vs hν plots for the CeO2 nanopowders prepared at 800,900,1100˚C sintering temperature respectively. The nature of the plots indicates a direct allowed transition. The values are found to be 3.66eV, 3.71eV and 3.78eV for the CeO2 nanopowders prepared at 800,900 and 1100˚C respectively [16]. It is found no significant change in the bandgap of the samples when increasing temperature.

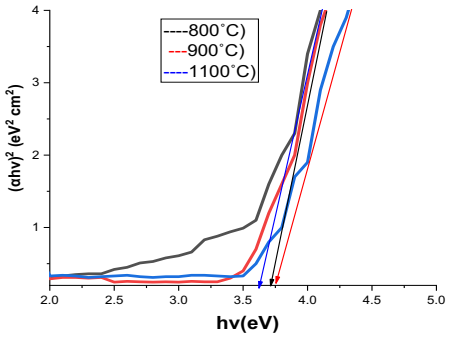

Fig.6: the dependence of αhν vs hν of CeO2 thin films prepared at 800, 900 and 1100 ˚C.

The charge transition occurred from (4f band) to the (valence band) leads to this phenomenon. The crystalline defects in the surface in the CeO2 nanoparticle samples lead to the emission of blue and greenish-blue color. All of the samples had different intensity values in the photoluminescence spectra because of the oxygen vacancies formed during the preparation process. The emission spectrum of a CeO2 sample sintering at 1100 ˚C is greater than that of CeO2 samples sintering at 800 and 900 ˚C. This could imply that the CeO2 sample sintering at 1100 degrees Celsius has superior crystallinity than the other samples.

4 Conclusion

Hydrothermal method is attractive method due to environment friendly, cost cheap and simple. It utilized to prepare CeO2 nanoparticle using Ce(III) acetate hydrate and Sodium hydroxide.The XRD patterns imply that the CeO2 cubic fluorite structure formed during the sintering of CeO2 samples at 800,900, and 1100 °C. The synthesized CeO2 samples are polycrystalline having the particle sizes of (32,37 and 47 nm). All the samples contain a weekly aggregation, while it is stronger at high temperatures due to the increase in density. As expected, the particle size ranges between 118- 122 nm at a temperature of 1100 ˚C. The spectra of all CeO2 samples show a broad band characteristic ranging from 320 to 535 nm. The cerium oxide (CeO2) sample sintering at 1100 ˚C has a strong bread UV emission band at 400 nm (3.12 eV). It can also be used to create nanoparticles of other intriguing materials. There is no significant change in energy band gap while the sintering temperature increased.

Conflict of Interest

All authors declare that there is no conflict of interest regarding the publication of this paper.

References

[1] S. Phokha , Thin Solid Films., **704**, 138001, 2020, doi: 10.1016/j.tsf.2020.138001.
[2] Hamed A Gatea,The role of substrate temperature on the performance of humidity sensors manufactured from cerium oxide thin films, Journal of Materials Science: Materials in Electronics, **31(24)**, 22119-22130,(2020)
[3] Hang Meng, Shihao Huang, and Yifeng Jiang, AIMS Materials Science., **7(5)**, 665–683,2020.
[4] T. An, X. Deng, S. Liu, S. Wang, J. Ju, and C. Dou, Ceram. Int.,**44(8)**,9742–9745,2018,doi: 10.1016/j.ceramint.2018.02.206.
[5 Y. J. Acosta-Silva et al., J. Nanomater., vol. 2019, 2019, doi: 10.1155/2019/5413134.
[6] X. Z. Song, W. Y. Zhu, X. F. Wang, and Z. Tan, ChemElectroChem.,**8(6)**,996–1020,2021,doi: 10.1002/celc.202001614.
[7] Hamed A Gatea, Iqbal S Naji, The effect of Ba/Sr ratio on the Curie temperature for ferroelectric barium strontium titanate ceramics, Journal of Advanced Dielectrics, **10(5)**,(2020).

[8] G. Jayakumar, A. A. Irudayaraj, and A. D. Raj, Mech. Mater. Sci. Eng. J., **9(2019)**, 2–7, 2017, doi: 10.2412/mmse.3.4.481.
[9] S. Soni, S. Kumar, B. Dalela, S. Kumar, P. A. Alvi, and S. Dalela, J. Alloys Compd., **752**, 520–531, 2018, doi: 10.1016/j.jallcom.2018.04.157.
[10] I. Kosacki, T. Suzuki, H. U. Anderson, and P. Colomban, Solid State Ionics., **149(1–2)**, 99–105, 2002, doi: 10.1016/S0167-2738(02)00104-2.
[11] Hamed A Gatea, Impact of sintering temperature on crystallite size and optical properties of SnO2 nanoparticles, Journal of Physics: Conference Series,**1829(1),** 2021.
[12] E. Swatsitang, S. Phokha, S. Hunpratub, and S. Maensiri, Phys. B Condens. Matter., **485**, 14–20, 2016, doi: 10.1016/j.physb.2016.01.002.
[13] H. Meng, S. Huang, and Y. Jiang, AIMS Mater. Sci.,**7(5)**, 665–683, 2020, doi: 10.3934/matersci.2020.5.665.
[14] M. Mittal, A. Gupta, and O. P. Pandey, Sol. Energy,165, March., 206–216, 2018, doi: 10.1016/j.solener.2018.03.033.
[15] I. T. Liu, M. H. Hon, and L. G. Teoh, Mater. Trans., **58(3)**,505–508,(2017),doi: 10.2320/matertrans.M2016285.
[16] A. Younis, D. Chu, and S. Li, Funct. Nanomater., 2016, doi: 10.5772/65937.